

INVESTIGATION OF THE $^{27}\text{Al}(\text{d}, \text{p})^{28}\text{Al}$ REACTIONAT $E_{\text{d}} = 12 \text{ MeV}$

T. P. G. CAROLA and J. G. VAN DER BAAN

Fysisch Laboratorium, Rijksuniversiteit, Utrecht, The Netherlands

Received 18 June 1971

Abstract: The $^{27}\text{Al}(\text{d}, \text{p})^{28}\text{Al}$ reaction has been investigated with a split-pole magnetic spectrograph at a bombarding energy of 12 MeV. The angular distributions of 41 proton groups have been measured. One new state has been found in ^{28}Al at an excitation energy of $3762 \pm 5 \text{ keV}$. Absolute spectroscopic factors have been determined by DWBA analysis. Some new I_{n} values are reported. The results are discussed within the framework of the shell model and comparison is made with recent many-particle calculations.

E NUCLEAR REACTION $^{27}\text{Al}(\text{d}, \text{p})$, $E = 12 \text{ MeV}$; measured $\sigma(\theta)$. ^{28}Al deduced levels, I , J^{π} , spectroscopic factors. Natural target.

1. Introduction

Stripping reactions have been extensively studied in the sd shell region but in the case of the $^{27}\text{Al}(\text{d}, \text{p})$ reaction the information is rather limited¹⁾. The reaction was previously studied at 6 MeV bombarding energy and PWBA theory was used to analyse the results. Moreover, the angular range of the proton distributions was limited to 5° – 60° which made the possible $I_{\text{n}} = 3$ distributions or admixtures uncertain. Finally, absolute reduced widths had been obtained by normalizing with less detailed results obtained at a different bombarding energy. For these reasons it appeared that it was necessary to investigate this reaction at a higher bombarding energy and with the use of DWBA theory. The results of this investigation are presented here.

A few years ago, shell-model calculations were performed for $A = 20$ – 28 nuclei [refs. ^{2, 16}]. In these calculations (set A hereafter), ^{16}O is taken as a closed core and the remaining particles occupy the $1\text{d}_{\frac{5}{2}}$ and $2\text{s}_{\frac{1}{2}}$ orbits. The two-body matrix elements were determined empirically from a set of known binding energies. These calculations yielded fair results for most of the nuclei under study but were rather unsuccessful for the doubly odd nuclei for which calculated energies differed from experimental values by 1 to 2 MeV. The results of more refined calculations were recently made available [ref. ¹⁶]] (set B hereafter), in which up to four holes in the $1\text{d}_{\frac{5}{2}}$ orbit and particles in the $2\text{s}_{\frac{1}{2}}$ and $1\text{d}_{\frac{3}{2}}$ orbits are considered. The surface-delta interaction was used to calculate the two-body matrix elements. The results of both calculations will be compared with experimental results.

2. Experimental procedure

A beam of 12 MeV deuterons from the 6 MV Utrecht tandem Van de Graaff accelerator bombarded a self-supporting target of natural aluminium of approximate thickness $50 \mu\text{g}/\text{cm}^2$. The reaction products were analysed in a split-pole magnetic spectrograph³⁾ and detected in an array of eight position-sensitive detectors (PSD) placed in the focal plane of the spectrograph. The $600 \mu\text{m}$ thick detectors, supplied by Nuclear Diodes, have a sensitive length of 30 mm (except for one which is 15 mm long) and a

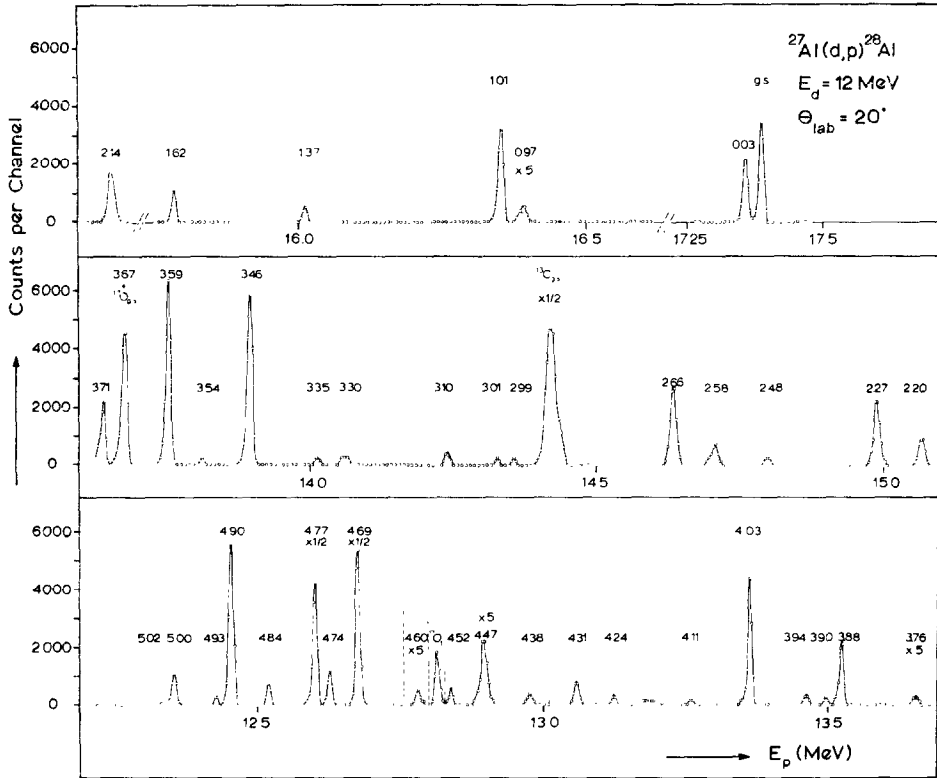


Fig. 1. A sample composite spectrum of two runs with different magnetic field settings taken with eight position-sensitive detectors in the focal plane of the split-hole spectrograph. In the regions between the peaks, the average of two consecutive channels was plotted. The peaks attributed to ^{28}Al are labelled by their excitation energy in MeV. The peaks labelled by $^{13}\text{C}_{\text{g.s.}}$, $^{17}\text{O}_{\text{g.s.}}$, and ^{17}O were caused by ^{12}C and ^{16}O , respectively, in the target. The total charge collected was $800 \mu\text{C}$ for each run.

height of 10 mm. Teflon foils with thicknesses ranging from 0.5 to 0.2 mm were placed in front of the detectors. The purpose of these foils is to absorb deuterons and α -particles, and also to decrease the energy of protons before detection. When a particle is detected, two signals are simultaneously produced: one "energy signal", E , propor-

tional to the energy loss of the incident particle and a "position signal", PE. After division of PE by E , it is possible to achieve high resolution even if the detector is too thin to stop the particles ⁴). A silicon detector placed in the scattering chamber at an angle of 60° with respect to the beam direction was used for monitoring purposes.

After amplification and routing ⁵), the data were sorted by means of a CDC 1700 computer ⁶). The raw data were also stored on magnetic tape to permit off-line analysis if necessary.

The angular distributions were measured in steps of 5° from $\theta = 5^\circ$ to 90° . The solid angle, delimited by the entrance slits of the spectrograph, was of the order of 1 msr for most of the runs. The PSD's were positioned in such a way that for each angle all the known proton groups corresponding to levels up to 5 MeV excitation could be detected in two runs with slightly different magnetic field settings.

The only strong contaminant groups were found to result from the (d, p) reaction on ^{12}C and ^{16}O . Very weak groups originating from $^{28}\text{Si}(\text{d}, \text{p})$ were also observed at small angles.

3. Results

A typical composite spectrum obtained at $\theta = 20^\circ$ is shown in fig. 1. Peaks from transitions to ^{28}Al levels are labelled by the excitation energy (in MeV) of the corresponding levels. The proton groups originating from contaminants were identified by their kinematic shift with respect to the ^{28}Al groups as well as by their position in the focal plane of the spectrograph. In this way, it was also possible to determine the presence of a new level in ^{28}Al as the corresponding proton group does not shift with respect to the ^{28}Al groups for the whole angular range. The excitation energy of this level was measured as 3762 ± 5 keV by linear interpolation between the excitation energies corresponding to the closest known groups. Except for this level no attempt was made to determine the excitation energies of ^{28}Al states accurately as most of these energies are already known with great accuracy from γ -ray work ⁷⁻¹⁰). The average FWHM is of the order of 11 keV. It must be pointed out that the background in this spectrum is extremely low. Evaluated for the strong peaks, the peak to background ratio is of the order of 1500 for the whole range. All the peaks of interest, even those weakly excited, are well defined. The protons feeding the ground-state doublet have an energy of ≈ 13.8 MeV after slowing down through the 0.5 mm thick teflon foil, whereas the PSD's will only stop protons up to $E_p = 11$ MeV.

Absolute cross sections were obtained by normalizing the measured yields with the aid of the yield of 4 MeV deuterons elastically scattered by the same target and with the same geometry for angles $\theta \leq 25^\circ$. In this case, it is assumed that Coulomb scattering dominates. This assumption is certainly correct as previous measurements ¹⁷) have shown it to be true for $^{28}\text{Si}(\text{d}, \text{d})$ for angles up to 30° and deuteron energies up to 4 MeV.

The angular distributions of protons feeding 42 states in ^{28}Al have been measured. The results are shown in figs. 2-7. It must be pointed out that the proton group feeding

the state labelled 1.62 MeV corresponds in fact to a close doublet of levels at $E_x = 1620$ and 1623 keV [ref. ⁸]).

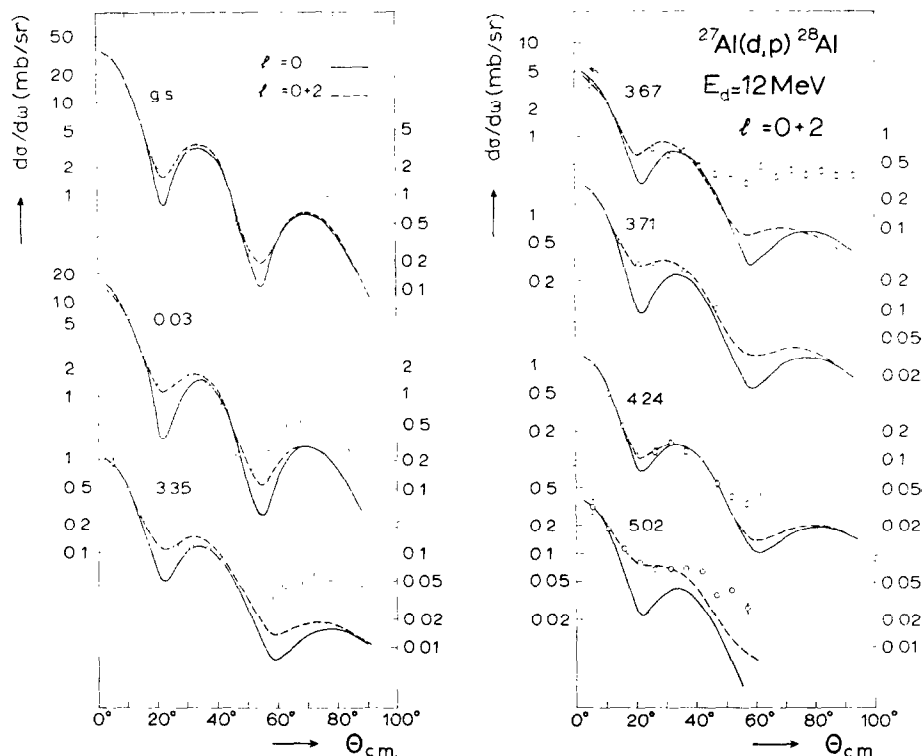


Fig. 2. Experimental differential cross sections for the $^{27}\text{Al}(\text{d}, \text{p})$ reaction. Statistical errors have been indicated if exceeding the dot size. An additional 5% error is introduced by the normalization procedure. The solid lines are the results of DWBA calculations for $l_n = 0$, the dotted lines are the results of DWBA calculations for $l_n = 0+2$, using the calculation for $1d_{3/2}$ particle transfer for the $l_n = 2$ component.

4. Analysis

The code DWUCK was used to calculate DWBA differential cross sections to be compared with experimental angular distributions in order to extract spectroscopic factors. The calculations were performed on an IBM 360 computer at the Technische Hogeschool in Delft. In order to limit the amount of computing time, the different DWBA distributions were calculated for a limited number of states with excitation energies differing by at most 500 keV. The DWBA curves for states in between were obtained by interpolation.

The values of the optical-model parameters for the deuteron, proton and neutron used in the DWBA calculations were obtained from previously published results ^{12, 13}).

They are given in table 1. Spin-orbit coupling was included in the optical potentials. A finite range of 0.621 fm was used in all calculations. The parameters used in the non-local potential correction were 0.85 fm for the proton and 0.54 fm for the deuteron.

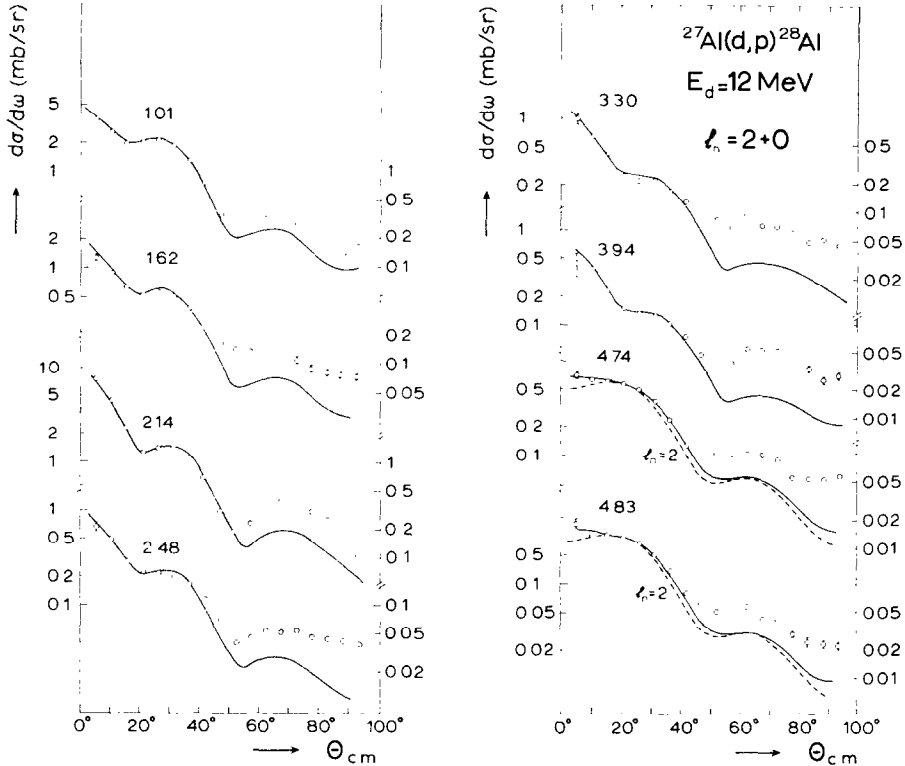


Fig. 3. Experimental differential cross sections. The solid lines are the results of DWBA calculations for $l_n = 2+0$. Also see caption of fig. 2.

The experimental cross section is defined by

$$\frac{d\sigma}{d\Omega} = 1.53 [(2J_f + 1)/(2J_i + 1)] S_n \sigma_{\text{DWBA}}(\theta),$$

where J_i and J_f are the spins of the target and residual nuclei, respectively.

As the reaction studied here involves an odd- A target, some proton angular distributions may be due to an incoherent mixture of transferred waves of the same parity corresponding to orbital angular momenta differing by two units. The angular distributions were fitted with the DWBA predictions by means of a least-squares program allowing the contribution of two l_n values as well as the addition of a constant background corresponding to the compound nucleus (CN) contribution. In order to have

an estimate of the CN contribution, some calculations were performed with a Hauser-Feshbach program. For the levels of interest, except for the 0.97 MeV (0^+) level, the CN cross sections were estimated to be isotropic and of the order of $10\text{--}20\ \mu\text{b/sr}$. For the 0.97 MeV state, the calculated CN contribution is shown in fig. 6. For the four angular distributions which do not exhibit a marked stripping pattern (fig. 7), it can only be said that the cross sections are of the same order of magnitude as the calculated CN cross sections.

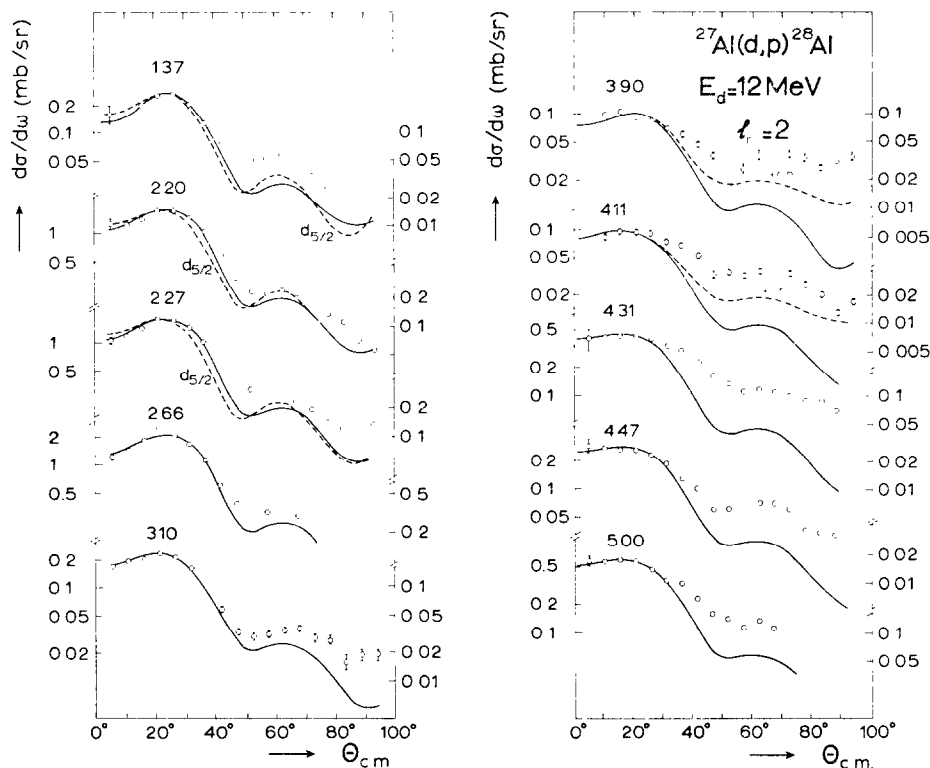


Fig. 4. Experimental differential cross sections. The solid lines are the results of DWBA calculations for $l_n = 2$ corresponding to $1d_{5/2}$ particle transfer. Also see caption of fig. 2.

For the sake of completeness, the values of $(2J_f + 1)S_n$ shown in table 2 are given for both values of the spin of the transferred neutron for each l_n value, except for $2p_{3/2}$ and $2p_{1/2}$ transfers for which the $(2J_f + 1)S_n$ values differ by less than 1%. The spectroscopic factors have relative errors of the order of 10 to 15%. However, there may be large systematic errors introduced by the particular choice of optical model parameters.

5. Discussion

Most of the l_n values assigned on the basis of PWBA analysis¹⁾ have been confirmed here. There are however some disagreements. A definite $l_n = 2$ transfer for

the 4.83 MeV state is in contradiction with the previous $I_n = 1$ assignment. Values of $I_n = 0$ transfers have previously been suggested for the levels at 4.52 and 4.60 MeV. The proton angular distributions obtained for these levels are shown in fig. 7. They apparently do not exhibit any stripping pattern but it must be pointed out that the 5° measurements are unfortunately missing. Nevertheless, if an $I_n = 0$ transfer were assigned to these angular distributions, one would obtain very small $I_n = 0$ spectroscopic factors.

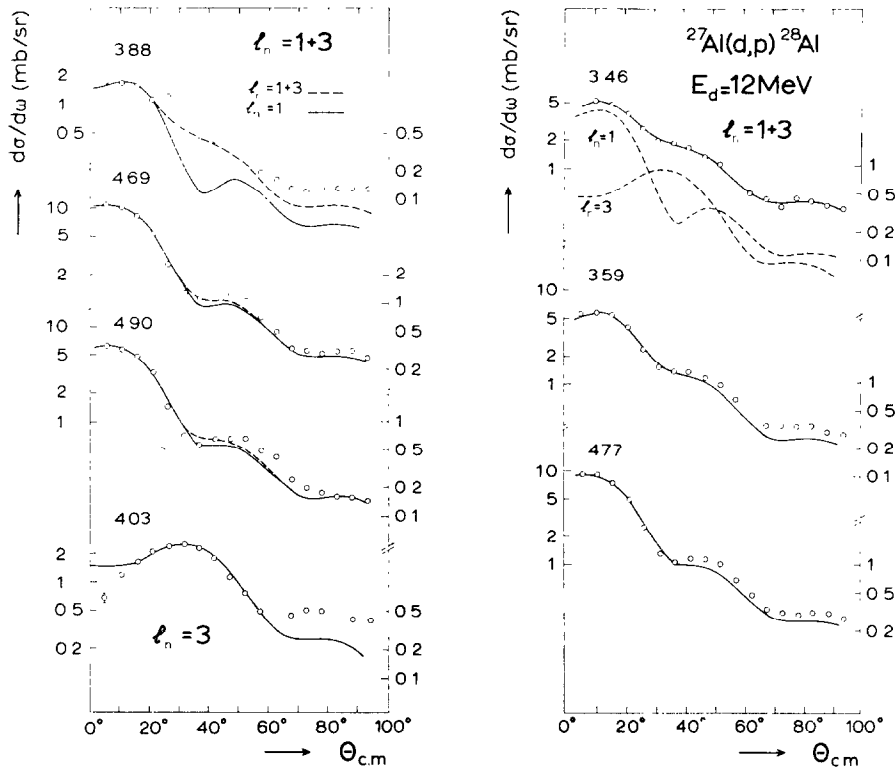


Fig. 5. Experimental differential cross sections for odd-parity cases. The upper three distributions on the left correspond to dominant $I_n = 1$ transfer. In all cases the $I_n = 3$ components correspond to $1f_{7/2}$ particle transfer. Also see caption of fig. 2.

Absolute reduced widths θ^2 as obtained from the previous PWBA analysed (d, p) work and spectroscopic factors S_n are related by $\theta^2 = S_n \theta_0^2$, where the single-particle widths θ_0^2 are proportional to the square of the radial wave function $R_{nl}(r_0)$ evaluated at the nuclear surface. In order to compare the previously published θ^2 values to the present spectroscopic factors, the θ_0^2 values have been taken from empirical graphs published in ref. ¹¹). The results are shown in table 2. The agreement is fair for the positive-parity states but poor for the negative parity states. For the mixed $I_n = 1+3$ transitions, this is explainable because the $I_n = 3$ contributions were not given in

ref. ¹). For pure $l_n = 1$ transitions, the $(2J_f + 1)\theta^2/\theta_0^2$ values are too large compared to $(2J_f + 1)S_n$. This systematic trend could imply that the $\theta_0^2 = 0.025$ value used in the calculations is too small.

TABLE I
Optical-model parameters used in the DWBA calculations

| | E (MeV) | V (MeV) | r_0 (fm) | a_0 (fm) | W_D (MeV) | r_{01} (fm) | a_{01} (fm) | r_{0c} (fm) | V_s (MeV) |
|-----------------|--------------|--------------|---------------|---------------|----------------|------------------|------------------|------------------|-----------------------|
| d ^{a)} | 11.8 | 91.0 | 1.20 | 0.79 | 27.4 | 1.55 | 0.46 | 1.30 | 9.9 |
| p ^{b)} | 21.2 | 45.7 | 1.20 | 0.64 | 8.2 | 1.07 | 0.60 | 1.30 | 6.4 |
| n | | | 1.25 | 0.65 | | | | 1.30 | $\lambda_{s.o.} = 25$ |

^{a)} Ref. ¹²).

^{b)} Ref. ¹³).

Below $E_x = 3.4$ MeV, all the states have positive parity. The ground state doublet of ^{28}Al shares most of the $l_n = 0$ strength and could be described by the configuration $(d_{\frac{3}{2}}^{-1}s_{\frac{3}{2}})_{J=2,3, T=1}$. Similarly, the states with large $l_n = 2$ strengths are expected to be mainly described by $d_{\frac{3}{2}}^{-1}d_{\frac{3}{2}}$ configurations.

Two $J^\pi = 1^+$ states at 1.37 and 1.62 MeV excitation are fed by allowed β^- transitions from ^{28}Mg [ref. ⁷]. Assuming the main configuration of the ground state of ^{28}Mg to be $(d_{\frac{3}{2}}^{-2}s_{\frac{3}{2}}^2)_{J=0, T=2}$ results in a configuration $(d_{\frac{3}{2}}^{-2}s_{\frac{3}{2}}^2)_{J=1, T=1}$ for the daughter states ⁸). To explain the $l_n = 2$ transfer to these states in the $^{27}\text{Al}(\text{d}, \text{p})$ reaction, one must then assume a $d_{\frac{3}{2}}^{-1}s_{\frac{3}{2}}^2$ admixture in the ^{27}Al ground state. This admixture would also explain the probable $l_n = 2$ transfer to the 0.97 MeV (0^+) state in ^{28}Al . These examples show that configuration mixing is to be expected in the description of ^{28}Al states. It would then be of interest to know the amount of $l_n = 2$ transfer corresponding to the $1d_{\frac{3}{2}}$ and $1d_{\frac{5}{2}}$ orbits, which could be done with a polarization sensitive experiment.

Between $E_x = 3.4$ and 5.0 MeV, seven levels have negative parity resulting from $l_n = 1$, $l_n = 3$ or $l_n = 1+3$ transfers. Among these, the 3.46 MeV state has been assigned $J^\pi = 4^-$ and the 3.59 MeV state $J^\pi = 4^-$ (2^-) from (n, γ) γ -ray circular polarization measurements ¹⁵). No spin assignment has yet been made to the 3.88 MeV state, for which the $l_n = 1$ transfer only limits J^π to $(1-4)^-$. This state decays mainly to the (3^+) ground state and also to the 1.62 MeV (1^+) state ⁹). If one assumes that this state is most likely to decay via an E1 transition, then only $J^\pi = 2^-$ would remain. In a recent study of the $^{27}\text{Al}(\text{p}, \gamma)$ reaction ¹⁴), the 1519 keV resonance with $J^\pi = 2^-$ is thought to correspond to the analogue of the 3.88 MeV state in ^{28}Al . The $J^\pi = 2^-$ assignment is in agreement with the above conclusion. The same study of analogue resonances in ^{28}Si also agrees with the $J^\pi = 4^-$ assignment to the 3.46 MeV state ($E_p = 1118$ keV) but would indicate $J^\pi = 3^-$ for the 3.59 MeV state ($E_p = 1199$ keV). The $E_p = 1724$ keV resonance probably corresponds to the analogue of the 4.03 MeV state and suggests $J^\pi = 5^-$ for this state. The states with large $l_n = 3$ strength are expected to be members of the $(1d_{\frac{3}{2}}^{-1}1f_{\frac{7}{2}})_{J=1-6}$ sextuplet. Under the as-

TABLE 2
Spectroscopic factors and I_n values for the $^{27}\text{Al}(\text{d}, \text{p})^{28}\text{Al}$ reaction

| $E_x^a)$ (MeV) | Previous work ^{c)} | | $(2J_f+1)S_n^d)$ | | | | This experiment | | | | Theory ^{e)} $(2J_f+1)S_n$ $I_n = 0$ $I_n = 2$ | |
|-------------------|-----------------------------|-------|------------------|-------|--------------------|--------------------|--------------------|---------------------------------|--------------------|--------------------|--|--------------------|
| | $J^{\pi b)}$ | I_n | $(2J_f+1)S_n^d)$ | I_n | $(2J_f+1)S_n$ | | | | | | | |
| | | | | | $2s_{\frac{1}{2}}$ | $1d_{\frac{3}{2}}$ | $1d_{\frac{5}{2}}$ | $2p_{\frac{1}{2}, \frac{3}{2}}$ | $1f_{\frac{7}{2}}$ | $1f_{\frac{5}{2}}$ | | |
| 0 | 3^+ | 0 | 3.75 | 0+2 | 4.30 | 0.80 | 1.20 | | | | 4.60 | 0.68 |
| 0.031 | 2^+ | 0 | 2.50 | 0+2 | 2.00 | (0.20) | 1.10 | | | | 2.76 | 0.53 |
| 0.972 | 0^+ | | | (2) | | | | | | | | 0.15 |
| 1.014 | 3^+ | 2+0 | 4.80, 0.6 | 2+0 | 0.44 | 5.70 | 7.45 | | | | 0.12 | 2.39 |
| 1.373 | 1^+ | 2 | | 2 | | 0.60 | 0.85 | | | | | 0.18 |
| 1.620 | 1^+ | } | | | 0.16 | 1.20 | 1.35 | | | | | 0.18 |
| 1.623 | $(2, 3)^+$ | | 0+2 | | | | | | | | 0.07 ^{f)} | 1.55 ^{f)} |
| 2.138 | $(2, 3)^+$ | | 1.25 | 0+2 | 0.75 | 2.25 | 2.70 | | | | | 0.04 |
| 2.202 | 1^+ | 2 | 1.48 | 2 | | 1.40 | 2.10 | | | | | |
| 2.272 | $(2-4)^+$ | 2 | 4.07 | 2 | | 3.20 | 4.70 | | | | | |
| 2.485 | 2^+ | 0+(2) | 0.25 | 0+2 | 0.08 | 0.40 | 0.48 | | | | | |
| 2.582 | | | | (0+2) | (0.05) | (1.06) | (1.30) | | | | | |
| 2.656 | $(1-5)^+$ | 2 | 4.07 | 2 | | 4.45 | 4.85 | | | | | |
| 2.987 | | | | (2) | | (0.14) | (0.18) | | | | | |
| 3.011 | $(0-5)^+$ | 2 | | 2 | | 0.14 | 0.20 | | | | | |
| 3.103 | $(0-4)^+$ | 2 | | 2 | | 0.40 | 0.50 | | | | | |
| 3.296 | $(2, 3)^+$ | 0+(2) | 0.12 | 0+2 | 0.13 | 0.24 | 0.26 | | | | | |
| 3.347 | $(2, 3)^+$ | 0 | 0.10 | 0+2 | 0.11 | 0.11 | 0.12 | | | | | |
| 3.465 | 4^- | 1+(3) | 3.20 | 1+3 | 0.11 | 0.11 | 0.12 | | | | | |
| 3.537 | | | | (2) | | (0.06) | (0.07) | | | | 9.10 | |
| 3.591 | $4^-, (2^-)$ | 1+(3) | 5.20 | 1+3 | | | | | | | | |
| 3.669 | $(2, 3)^+$ | 0 | 0.05 | 0+2 | 0.04 | 0.11 | 0.13 | | | | 6.00 | |

| | | | | | | | | | | |
|--------|------------------------------------|-------|------|-------|--------|--------|--------|------|------|------|
| 3.706 | (2, 3) ⁺ | 0 | 0.20 | 0+2 | 0.20 | 0.31 | 0.38 | | | |
| 3.762 | | | | | | | | | | |
| 3.876 | (1-4) ⁻ | 1 | 1.20 | 1+3 | | | | | | |
| 3.900* | (0-5) ⁺ | (2) | | 2 | | | | | | |
| 3.936 | (2, 3) ⁺ | 0+2 | | 0+2 | 0.06 | 0.12 | 0.15 | 0.37 | 1.35 | 1.50 |
| 4.033* | (0-6) ⁻ | (3) | | 3 | | | | | | |
| 4.115 | (0-5) ⁺ | 2 | | 2 | | 0.12 | 0.17 | | 9.30 | 12.9 |
| 4.243 | (2, 3) ⁺ | 0 | 0.10 | 0+2 | 0.12 | 0.04 | 0.06 | | | |
| 4.315 | (0-5) ⁺ | 2 | 1.10 | 2 | | 0.50 | 0.62 | | | |
| 4.383 | | | | | | | | | | |
| 4.466* | (0-5) ⁺ | 2 | | 2 | | 0.30 | 0.36 | | | |
| 4.518 | | (0) | | n.a. | | | | | | |
| 4.598 | | (0) | | n.a. | | | | | | |
| 4.691 | 2 ⁻ , (3 ⁻) | 1 | 3.20 | 1+3 | | | | 2.20 | 0.55 | 1.0 |
| 4.739 | (0, 5) ⁺ | 2 | | (0)+2 | (0.03) | 0.50 | 0.56 | | | |
| 4.766 | (2, 3) ⁻ | 1+(3) | 2.55 | 1+3 | | | | 2.05 | 0.75 | 1.10 |
| 4.835* | (0-5) ⁺ | 1 | | (0)+2 | (0.01) | 0.25 | 0.30 | | | |
| 4.905 | (2, 4) ⁻ | 1 | 3.20 | 1+3 | | | | 1.20 | 0.30 | 0.45 |
| 4.928 | | | | (0+2) | (0.01) | (0.09) | (0.11) | | | |
| 4.999 | (0-5) ⁺ | 2 | | 2 | | 0.45 | 0.56 | | | |
| 5.019 | (2, 3) ⁺ | 0 | | 0+2 | 0.04 | 0.05 | 0.06 | | | |

a) Excitation energies from refs. 1, 7-10, except for the 3.76 MeV level which has been first observed in the present work (see sect. 3).

b) From refs. 1, 7, 8, 15) with additional information (indicated with an asterisk) from the present work.

c) Ref. 1).

d) See sect. 5.

e) Ref. 16).

f) Assuming $J = 3$ for this state.

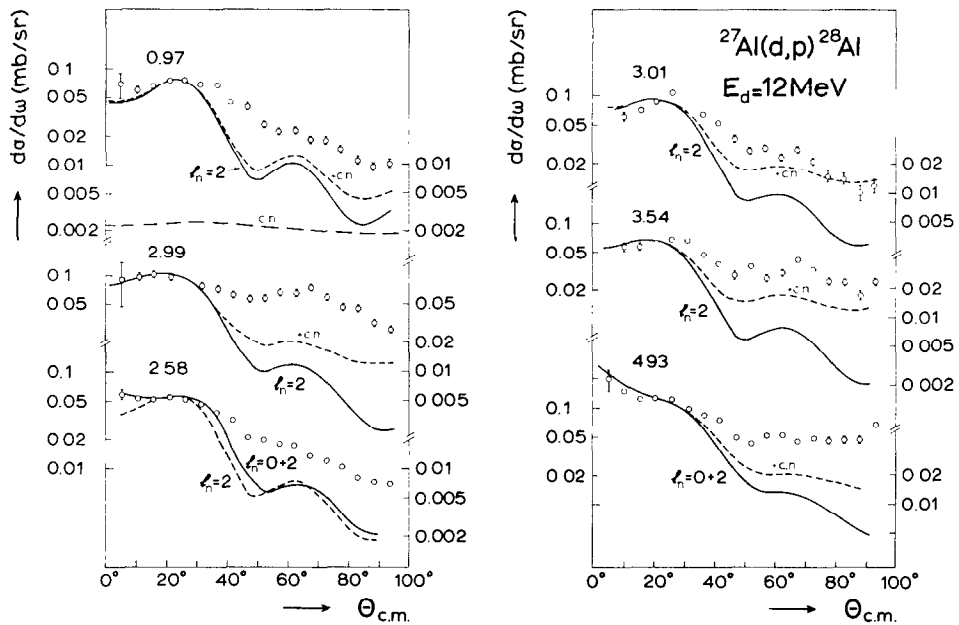


Fig. 6. Experimental differential cross sections with probable $l_n = 2$ or $l_n = 2+0$ transfer. For the 0.97 MeV state distribution, the solid line corresponds to $1d_{3/2}$ particle transfer. For all the other distributions the $l_n = 2$ component is the calculated DWBA distribution for $1d_{3/2}$ particle transfer. In most cases, the compound nucleus contribution has been added to the DWBA distribution (see sect. 4). Also see caption of fig. 2.

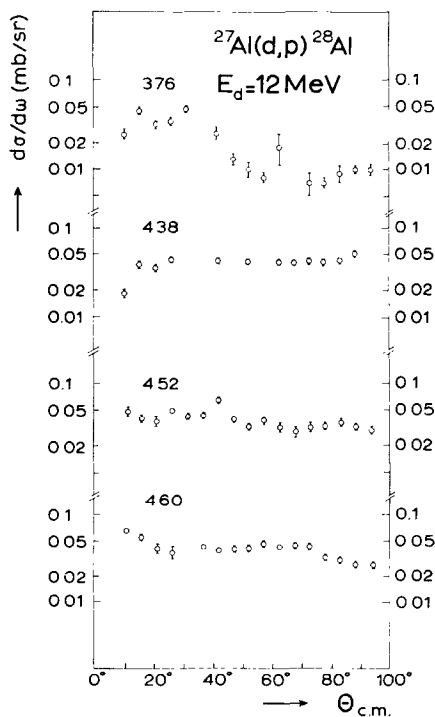


Fig. 7. Experimental differential cross sections which could not be fitted by DWBA calculations. Also see caption of fig. 2.

sumption that the above spin assignments are correct, S_n values for the negative-parity states are shown in table 3. Only the 4.03 MeV (5^-) state has almost full single-particle strength. There is a fragmentation of the remaining single-particle states as well as mixing with $1\text{d}_{\frac{3}{2}}^{-1}2\text{p}$ states.

TABLE 3
The S_n values for negative-parity states of ^{28}Al below $E_x = 5.0$ MeV

| E_x (MeV) | J^π ^{a)} | S_n | |
|----------------|-----------------------|-----------------|---------------------------|
| | | 2p | $1\text{f}_{\frac{7}{2}}$ |
| 3.46 | 4^- | 0.11 ± 0.02 | 0.62 ± 0.09 |
| 3.59 | 3^- | 0.19 ± 0.03 | 0.60 ± 0.09 |
| 3.88 | 2^- | 0.07 ± 0.01 | 0.27 ± 0.04 |
| 4.03 | 5^- | | 0.85 ± 0.17 |
| 4.69 | 2^- | 0.44 ± 0.07 | 0.11 ± 0.02 |
| 4.77 | 2^- | 0.41 ± 0.06 | 0.15 ± 0.02 |
| | 3^- | 0.29 ± 0.04 | 0.11 ± 0.02 |
| 4.90 | $(2-4)^-$ | | |

^{a)} Suggested spin assignment (see sect. 5).

TABLE 4
Comparison between experimental and calculated excitation energies and spectroscopic factors for the low-lying states of ^{28}Al ^{a)}

| J^π | E_x (MeV) | | | S_n for $l_n = 0$ | | | S_n for $l_n = 2$ | | |
|---------|-------------|-------|-------|---------------------|------|------|---------------------|-------|-------|
| | exp. | A | B | exp. | A | B | exp. ^{b)} | A | B |
| 3^+ | 0 | 0 | 0 | 0.62 ± 0.09 | 0.04 | 0.66 | 0.14 ± 0.05 | 0.10 | 0.10 |
| 2^+ | 0.03 | -2.81 | 0.08 | 0.40 ± 0.06 | 0.43 | 0.39 | 0.18 ± 0.07 | 0.12 | 0.08 |
| 0^+ | 0.97 | -3.44 | -0.18 | | | | 0.20 ± 0.05 | 0.49 | 0.15 |
| 3^+ | 1.01 | 1.74 | 1.94 | 0.06 ± 0.01 | 0.56 | 0.02 | 0.96 ± 0.26 | 0.009 | 0.34 |
| 1^+ | 1.37 | -0.40 | 0.74 | | | | 0.11 ± 0.03 | 0.49 | 0.023 |

^{a)} See sect. 1 for the definition of sets A and B.

^{b)} The S_n values for $1\text{d}_{\frac{3}{2}}$ and $1\text{d}_{\frac{5}{2}}$ transfer have been averaged.

The theoretical calculations described in sect. 1 are compared with experimental results in table 4. Although there are still discrepancies between calculated and measured excitation energies when the $1\text{d}_{\frac{3}{2}}$ orbit is included in the calculations (set B), there is a definite improvement in the calculated spectroscopic factors. The theoretical results from set B have been compared with experiment in table 2. The measured $(2J_f + 1)S_n$ values are well reproduced for the first three states whereas only qualitative agreement is achieved for the next four states. For $E_x > 2.20$ MeV, calculated $(2J_f + 1)S_n$ values have not been compared with experiment because experimentally many spin assignments are missing. It can only be said that the large strengths observed for some states are not reproduced by the theoretical calculations.

In conclusion, although definite improvement has been brought about by the inclusion of the $1d_{3/2}$ orbit in the theoretical calculations, an even larger shell-model space may be needed to accurately describe ^{28}Al . This however would result in prohibitive matrix size and is not feasible for the time being.

We would like to thank Dr. P. W. M. Glaudemans for suggesting this work and for his constant interest. We also thank Prof. P. M. Endt, Prof. A. M. Hoogenboom and Dr. C. van der Leun for many valuable discussions and for their critical reading of the manuscript. We wish to thank Dr. B. H. Wildenthal for communicating the results of his calculations. The help of J. C. van der Weerd and J. G. Tamboer is gratefully acknowledged.

This investigation was partly supported by the joint program of the "Stichting voor Fundamenteel Onderzoek der Materie" and the "Nederlandse Organisatie voor Zuiver Wetenschappelijk Onderzoek".

References

- 1) P. M. Endt and C. van der Leun, Nucl. Phys. **A105** (1967) 1
- 2) B. H. Wildenthal, J. B. McGrory, E. C. Halbert and P. W. M. Glaudemans, Phys. Lett. **26B** (1968) 692
- 3) J. E. Spencer and H. A. Enge, Nucl. Instr. **49** (1967) 181
- 4) P. H. Debenham, D. Dehnhard and R. W. Goodwin, Nucl. Instr. **67** (1967) 288
- 5) A. C. Wolff and H. G. Leighton, Nucl. Phys. **A140** (1970) 319
- 6) J. G. van der Baan and H. G. Leighton, Nucl. Phys., **A170** (1971) 607
- 7) D. E. Alburger and W. R. Harris, Phys. Rev. **185** (1969) 1495
- 8) D. O. Boerma, Thesis, Groningen (1970)
- 9) R. M. Freeman and A. Gallmann, Nucl. Phys. **A156** (1970) 305
- 10) R. Hardell, S. O. Idetjärn and H. Ahlgren, Nucl. Phys. **A126** (1969) 392
- 11) M. H. MacFarlane and J. B. French, Rev. Mod. Phys. **32** (1960) 567
- 12) G. D. Jones, R. R. Johnson and R. J. Griffiths, Nucl. Phys. **A107** (1968) 659
- 13) R. W. Barnard and G. D. Jones, Nucl. Phys. **A108** (1968) 655
- 14) A. Tveter, Oslo University, private communication
- 15) F. Stecher-Rasmussen, K. Abrahams and J. Kopecky, Reactor Centre, Petten, Nucl. Phys., to be published
- 16) B. H. Wildenthal, Michigan State University, private communication
- 17) H. E. Gove *et al.*, Nucl. Phys. **A116** (1968) 369